Journal of Alloys and Compounds 488 (2009) 27–30

Contents lists available at ScienceDirect

Journal of Alloys and Compounds

journal homepage: www.elsevier.com/locate/jallcom

Exchange bias effect at the irregular interfaces between Co and CoO nanostructures

S. Das, M. Patra, S. Majumdar, S. Giri*

Department of Solid State Physics, Indian Association for the Cultivation of Science, Jadavpur, Kolkata 700 032, India

ARTICLE INFO

Article history:
Received 27 May 2009
Received in revised form 28 August 2009
Accepted 31 August 2009
Available online 4 September 2009

Keywords:
Nanostructures
Sol–gel synthesis
Magnetic measurements
Exchange bias effect

ABSTRACT

Nanostructures of Co and CoO particles were synthesized by using a modified sol–gel technique. Coexistence of Co and CoO with *fcc* structure is identified by powder X-ray diffraction and electron diffraction studies. Particle sizes are found to be in between 4 nm and 13 nm obtained from Transmission Electron Microscopy where high resolution images do not reveal any regular core-shell structure; rather it shows a coexistence of Co and CoO nanostructure having irregular interfaces between them. A considerable shift in the magnetic hysteresis loop associated with the substantial enhancement of coercivity (from ~1.0 kOe to ~3.7 kOe) is observed at 5 K when the composite was cooled in field-cooled mode with a static cooling field, H_{cool} = 8 kOe. The shift in the hysteresis loop is the typical manifestation of exchange bias effect which is strongly dependent on the cooling field. The results reveal that substantial enhancement of coercivity is attributed to the strong exchange coupling at the irregular Co/CoO interfaces where strong exchange bias effect does not require any regular core-shell structure.

1. Introduction

Magnetic nanoparticles have drawn a considerable attention in the past decades for developing a more complete understanding of the fundamental properties in magnetism and technological applications in diverse areas such as magnetic storage materials, high-frequency magnetoelectric devices, biosensing materials, and drug delivery [1–8]. In fact, a high coercivity commensurate with the high magnetization is primarily desirable for many applications e.g., high density magnetic storage, development of hard magnet, magnetoelectric devices, etc. It has been observed that coercivity of the ferromagnetic nanoparticles having a critical size close to single magnetic domain is enhanced remarkably compared to that found in the bulk counterpart (e.g., Fe powder with a crystallite size of ~14 nm showed a coercivity of 1040 Oe [9] in comparison with ~0.9 Oe [10] for bulk Fe). Owing to their high coercivities the nanoscale crystallites have been recognized as potential candidates for the technological applications.

One of the promising strategies is to enhance the coercivity by exploiting exchange bias effect between two magnetic substances in a heterostructure [11–14]. Exchange bias effect is typically manifested by the systematic shift of the magnetic hysteresis loop in a magnetic heterostructure composed of ferromagnetic and antiferromagnetic substances when the system is cooled through the antiferromagnetic Néel temperature (T_N) in a static magnetic field [11]. The shift in the magnetic hysteresis loop defined as exchange bias field is typically associated with the enhancement of coercivity. The phenomenon of exchange bias is a topic that has been visited and revisited several times over the past 50 years since the discovery of exchange bias effect by Meiklejohn and Bean [11]. The reason is that there is an inherent complexity in varieties of structural combinations that lead to the competing interactions at the interface. Till date, a clear microscopic picture of the exchange bias effect at the ferromagnetic/antiferromagnetic interface is still remained elusive. Co/CoO having core/shell nanostructure is a model system for the exchange bias effect where Co is ferromagnetic and CoO is antiferromagnetic. Thus, the phenomenon of exchange bias effect has been revisited in Co/CoO nanostructures several times in different combinations of nanostructures and interfaces.

In this paper, we report the substantial increase of coercivity due to field cooling where the enhancement of coercivity is involved with the strong exchange coupling between ferromagnetic Co and antiferromagnetic CoO in a Co/CoO heterostructure. We observe a strong exchange bias effect without regular core-shell structure. A partial oxidation of Co particles having irregular interfaces between Co and CoO nanostructure are found to be sufficient for the substantial exchange bias effect.

2. Experimental section

Co/CoO nanostructure was synthesized by a modified sol–gel technique. The cobalt nitrate solution was prepared by dissolving cobalt powder (99.99%, Aldrich) in ~20% diluted nitric acid. The solution was transferred to a flask fitted with a

* Corresponding author. Tel.: +91 33 2473 4971; fax: +91 33 2473 2805.
E-mail address: sspsg2@iacs.res.in (S. Giri).

0925-8388/$ – see front matter © 2009 Elsevier B.V. All rights reserved.
doi:10.1016/j.jallcom.2009.08.143

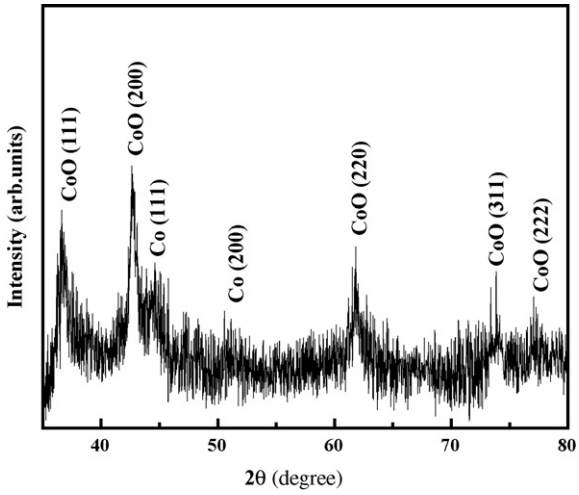

Fig. 1. Powder X-ray diffraction pattern displaying coexistence of *fcc* structure of Co and CoO nanoparticles.

condenser. A proper amount of citric acid (Loba Chemie 99.5%) was added to the cobalt nitrate solution and stirred for 4 h at 70 °C for achieving a homogeneous cobalt citrate solution. The amount of citric acid was so chosen to ensure that all the metal ions form metal citrate where only two of the citrate ions were considered to be taken part in the chemical bonding with the metal ions [15]. The clear solution was transferred to a borosil beaker and kept in an oil bath maintained at 80 °C for 36 h in air to slowly form a gel. Thermogram of thermogravimetric analyzer (TA instrument, SDT Q600) indicates that the decomposition of the dried gel was almost completed around ~300 °C by evolving a number of gases viz., CO, CO_2, NO_2, O_2, water vapour, etc. Thus, the final product was ground and calcined at 300 °C for 6 h in a flow of a gas consisting of a mixture of hydrogen (5%) and argon (95%). In situ oxygen partially oxidizes the Co nanoparticles which give rise to the Co and CoO nanostructures.

Crystalline phases of Co and CoO were identified by powder X-ray diffraction (XRD) with the CuK_α radiation ($\lambda = 1.5406$ Å) using a BRUKER axs D8 Advance diffractometer. Morphology, particle size, and size distribution of the particles were observed by the high resolution Transmission Electron Microscopy (TEM) using a JEOL JEM 2010 microscope operating at an accelerating voltage around 200 kV. The powdered sample was pressed into a pellet and a small part of the pellet was considered for the magnetization measurements. Magnetization measurements were carried out in a commercial cryogen-free high-field physical property measurement system (Cryogenics Ltd., UK).

3. Results and discussions

Fig. 1 depicts the powder XRD pattern of the sample recorded at room temperature which clearly indicates the coexistence of the diffraction patterns corresponding to *fcc* structure of Co and CoO with space group *Fm*3*m*. The diffraction pattern is consistent with those found in the JCPDS card (JCPDS 78-0431) for CoO and (JCPDS 10-0806) for Co. Any additional peak corresponding to Co_3O_4 and Co_2O_3 is absent in the XRD pattern. From the broadening of the diffraction peaks the average sizes of Co and CoO particles are estimated to be ~10 nm and ~13 nm, respectively using Scherrer formula [16] where the value is consistent with the higher limit of the range of particle size obtained from TEM image. Fig. 2(a) shows the TEM image of the dispersed particles. Histogram of the particle size having size distribution in between 4 nm and 13 nm is shown in the inset of Fig. 2(a) where the size distribution could be fitted with the log-normal distribution function, $f(d) = (2\pi)^{-1/2}(d\sigma)^{-1} \exp - [(\ln d - \ln d_0)^2/(2\sigma^2)]$. σ is the variance indicating the size distribution while d_0 is the mean size. The best fit according to the log-normal distribution function is shown in the inset of Fig. 2(a) by the continuous line with $d_0 = 6.4$ nm and $\sigma = 0.09$. The difference between TEM and XRD results may be ascribed to the different averaging processes of each technique while the number averaging is typically utilized in TEM and volume averaging is used in XRD. Fig. 2(b) shows the selected area electron diffraction of the nanoparticles which is in accordance with the crystalline state observed in the XRD pattern. An example of the high resolution TEM (HRTEM) image is shown in Fig. 2(c) showing the lattice fringes corresponding to Co and CoO nanostructures. The separation between consecutive lattice fringes is larger for CoO than Co. We note that Co and CoO nanostructures do not form a regular core-shell structure, although several attempts have been made to observe any core-shell structure. An example of the irregular interfaces between Co and CoO nanostructure is indicated by the broken line in the figure.

Field-cooled effect of magnetization was measured as a function of temperature where the arrows indicate the measurements in the warming and cooling cycles, respectively depicted in Fig. 3. The sample was first cooled down to 5 K from 300 K in zero-field, magnetization was measured in the warming cycle at 100 Oe for zero-field-cooled (ZFC) magnetization, and then magnetization was measured in the cooling cycle which gives us the field-cooled (FC) magnetization. The ZFC magnetization does not show any feature of blocking temperature in the temperature dependence even up to 300 K. An anomaly is noticed around ~285 K in Fig. 3 where antiferromagnetic Nèel temperature was reported for CoO [17]. In case of Co_3O_4 a peak corresponding to T_N at 30 K was observed [18] which is absent in the present observation indicating the absence of Co_3O_4. At 300 K a symmetric magnetic hysteresis loop is observed as shown in the inset of Fig. 3. Almost immeasurable coercivity is noticed at 300 K which may indicate that the measurement temperature is close to the superparamagnetic blocking temperature. We further note that magnetization at 50 kOe does not show any saturating tendency where the value (29 emu/g) is much smaller than the bulk value of Co having *fcc* structure with saturation magnetization, Ms ≈ 175 emu/g [19]. This discrepancy might be attributed to the various factors such as size effect, enhanced surface-to-volume ratio, and the presence of antiferromagnetic CoO [20].

Magnetic hysteresis loop was measured at 5 K in between ± 50 kOe after cooling the sample from 300 K in ZFC and FC modes shown in Fig. 4 by the continuous and broken lines, respectively. A considerably large shift in the hysteresis loop is observed for cooling the sample in FC mode which is the typical manifestation of exchange bias effect. Furthermore, a large enhancement of the coercivity is also noticed in the FC measurement. The values of the coercivity (H_C) and exchange bias field (H_E) are determined as $H_C = (H_2 - H_1)/2$ and $H_E = |(H_1 + H_2)|/2$. H_1 and H_2 are the left and right coercivities, respectively. The values of H_C and H_E at 5 K are ~3.9 kOe and ~3.0 kOe, respectively for the cooling field, $H_{cool} = 45$ kOe which are significantly large comparable to the reported values [20–23]. We strikingly note that a negative shift in the magnetic hysteresis loop is also present along the field axis shown in Fig. 4, although the sample was cooled in ZFC mode. In case of ZFC cooling a symmetric hysteresis loop without exchange bias effect is expected, despite very few reports are available where exchange field was reported even in ZFC mode [24]. In order to solve it we applied a large negative field at 300 K, then set the field to zero value, and finally the sample was cooled down to 5 K in ZFC mode. After stabilizing the temperature at 5 K the magnetic hysteresis loop was measured in between ± 50 kOe and a positive shift along the field axis is noted shown in Fig. 4. Since a large negative magnetic field was initially applied at 300 K and set it to zero value, a small negative residual field was present leading to the positive shift in the hysteresis loop. The residual magnetic field gives rise to the exchange bias effect manifested by the shift in the magnetic hysteresis loop even in case of cooling in ZFC mode. For negative residual field the shift is positive while it is negative for positive residual field.

In order to investigate cooling field dependence of the exchange bias effect the sample was cooled down to 5 K from 300 K in FC mode and H_E and H_C were measured at 5 K from the shift of the hysteresis loops by varying the cooling field. The values of H_E and H_C are displayed in Fig. 5 as a function of cooling field (H_{cool}). H_E is

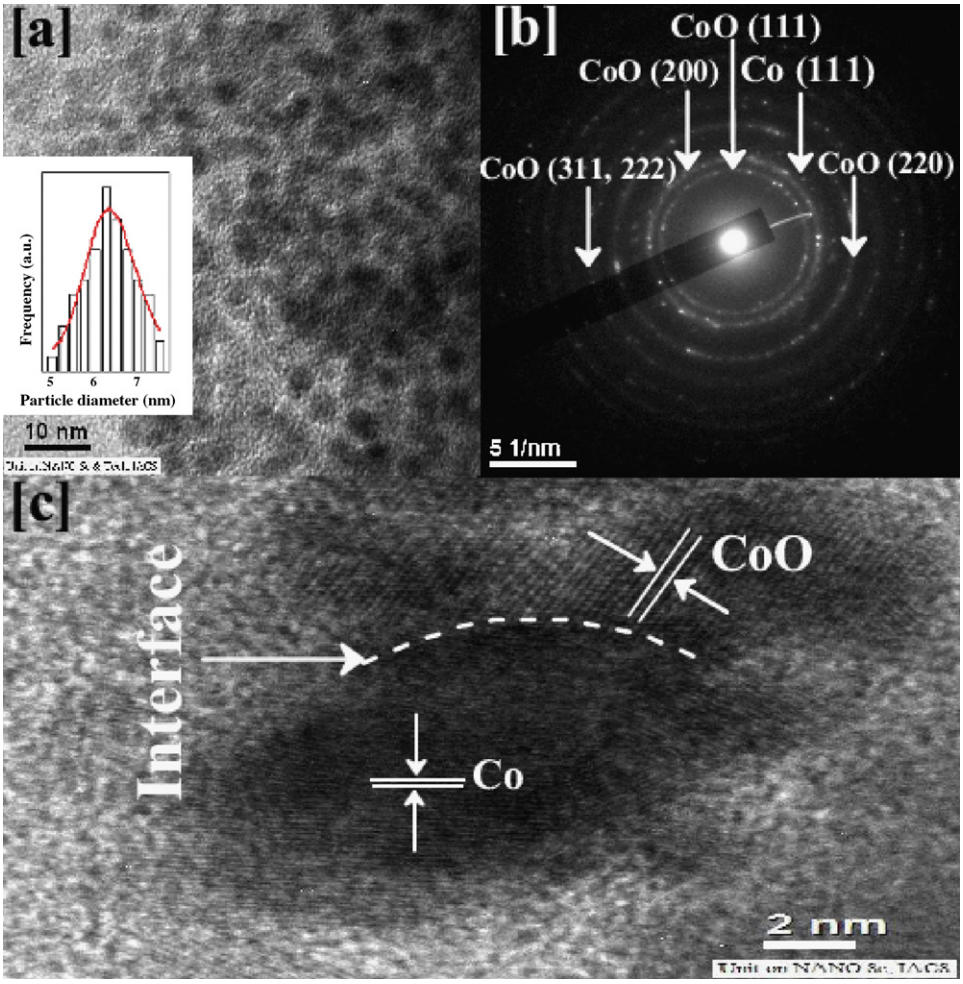

Fig. 2. (a) TEM image of the nanoparticles. Inset of (a): histogram of particle size distribution. (b) Electron diffraction having ring patterns corresponding to diffraction planes of the *fcc* structure of Co and CoO nanoparticles. (c) HRTEM image displaying the lattice fringes corresponding to Co and CoO. Interface area between Co and CoO is highlighted by the broken line.

increased to ~2.9 kOe associated with the substantial enhancement of coercivity at H_{cool} = 8 kOe and then both the parameters show a saturating trend for H_{cool} > 8 kOe. We note that H_C is enhanced up to ~3.7 kOe from ~1.0 kOe for H_{cool} = 8 kOe. In case of exchange bias phenomenon the system must contain two exchange coupled phases comprising of reversible and rigid phases where magnetization of the first one can be reversed and the second one cannot be reversed. Here, the ferromagnetic spins are reversible while the antiferromagnetic spins are rigid. In the case of field cooling the antiferromagnetic spins pin the ferromagnetic spins at the interface and form a new layer of pinned ferromagnetic spins which gives rise to the exchange bias effect. In the case of a low cooling

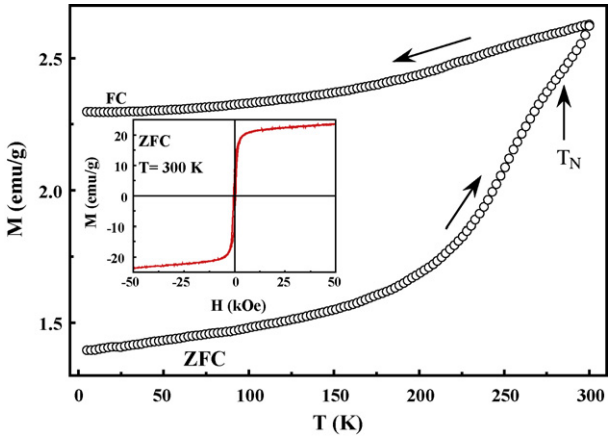

Fig. 3. Temperature dependence ZFC and FC magnetization curves taken at 100 Oe. Arrow indicates the Nèel temperature at T_N = 285 K. Inset: magnetic hysteresis loop at 300 K.

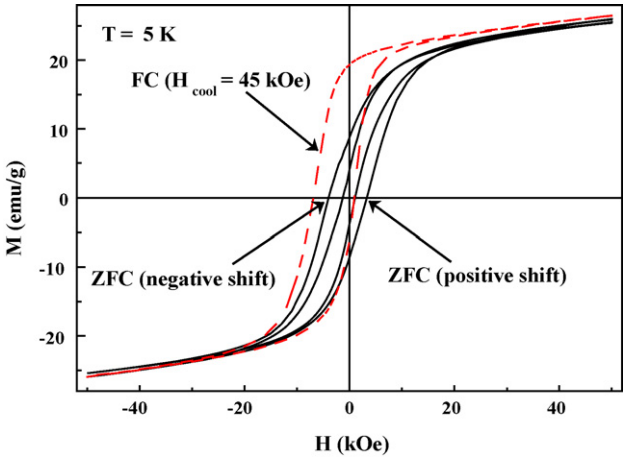

Fig. 4. Magnetic hysteresis loops at 5 K after cooling the sample in FC (H_{cool} = 45 kOe) and ZFC modes. For the ZFC modes the experimental protocol is described in the text.

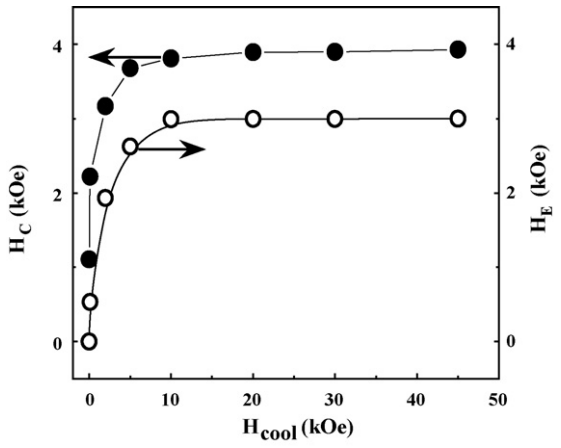

Fig. 5. Plot of coercivity (H_C) and exchange bias field (H_E) as a function of cooling field (H_{cool}) at 5 K.

field, H_{cool} is not strong enough to align the pinned ferromagnetic spins toward saturation. Therefore, the progressive alignment of the moment of the pinned ferromagnetic spins along the direction of H_{cool} is increased with increasing H_{cool} which reduces the effect of the averaging of the anisotropy due to randomness of spin alignment, resulting in the increase in effective anisotropy. Initially, a rapid increase in anisotropy is indicated by the sharp increase in H_C with H_{cool} as shown in Fig. 5. When the cooling field is high enough, the pinned ferromagnetic spins tend toward saturation and vary a little along the cooling field with the further increase in H_{cool}. Thus, H_E and H_C remain almost unchanged for $H_{cool} > 8$ kOe which is displayed in the figure.

4. Summary and conclusion

The nanostructure of Co and CoO particles was synthesized using a modified sol–gel technique. Crystalline phase of *fcc* structure with space group *Fm*3*m* of Co and CoO are identified by X-ray diffraction studies. Crystalline phase is further confirmed by the electron diffraction pattern of some selected portions of the particles. Particle sizes are found to be in between 4 nm and 13 nm obtained from the Transmission Electron Microscopy where high resolution images do not reveal any regular core-shell structure, rather it shows irregular interfaces between Co and CoO nanostructures.

Temperature dependence of magnetization does not show the feature of blocking temperature even at 300 K. A considerable shift in the magnetic hysteresis loop associated with the substantial enhancement of coercivity is observed at 5 K when the composite was cooled in field-cooled mode. The shift in the hysteresis loop is the typical manifestation of exchange bias effect which is strongly dependent on the cooling field. The results reveal that the substantial enhancement of coercivity is attributed to the strong exchange coupling between ferromagnetic Co and antiferromagnetic CoO at the irregular interfaces which does not require any regular core-shell structure.

Acknowledgements

S.G. wishes to thank DST (Project No. SR/S2/CMP-46/2003), India for the financial support. S.D. wishes to thank CSIR, India for the JRF fellowship.

References

[1] S.D. Bader, Rev. Modern Phys. 78 (2006) 1.
[2] A.H. Lu, E.L. Salabas, F. Schüth, Angew. Chem. Int. Ed. 46 (2007) 1222.
[3] D.L. Leslie-Pelecky, R.D. Rieke, Chem. Mater. 8 (1996) 1770.
[4] M.C. Urbina, S. Zinoveva, T. Miller, C.M. Sabliov, W.T. Monroe, C.S.S.R. Kumar, J. Phys. Chem. C 112 (2008) 11102.
[5] N. Cordente, M. Respaud, F. Senocq, M.J. Casanove, C. Amiens, B. Chaudret, Nano Lett. 1 (2001) 565.
[6] V.F. Puntes, K.M. Krishnan, A.P. Alivisatos, Science 291 (2001) 2115.
[7] R.H. Kodama, J. Magn. Magn. Mater. 200 (1999) 359.
[8] J. Zhang, C. Boyd, W. Luo, Phys. Rev. Lett. 77 (1996) 390.
[9] S. Gangopadhyay, G.C. Hadjipanayis, B. Dale, C.M. Sorensen, K.J. Klabunde, V. Papaefthymiou, A. Kostikas, Phys. Rev. B 45 (1992) 9778.
[10] R.M. Bozorth, Ferromagnetism, D. Van Nostrand Company, Inc., New York, 1951.
[11] W.H. Meiklejohn, C.P. Bean, Phys. Rev. 102 (1956) 1413.
[12] J. Nogues, J. Sort, V. Langlais, V. Skumryev, S. Surinach, J.S. Munoz, M.D. Baro, Phys. Rep. 422 (2005) 65;
J. Nogues, J. Sort, V. Langlais, V. Skumryev, S. Surinach, J.S. Munoz, M.D. Baro, Int. J. Nanotechnol. 2 (2005) 23;
J. Nogues, I.K. Schuller, J. Magn. Magn. Mater. 192 (1999) 203.
[13] S.B. Darling, S.D. Bader, J. Mater. Chem. 15 (2005) 4189.
[14] O. Iglesias, A. Labarta, X. Batlle, J. Nanosci. Nanotechnol. 8 (2008) 2761.
[15] R.N. Panda, J.C. Shih, T.S. Chin, J. Magn. Magn. Mater. 257 (2003) 79.
[16] B.D. Cullity, Elements of X-ray Diffractions, Addison-Wesley Publishing Company, Inc., 1978 (Reading).
[17] J. Sakurai, W.J.L. Buyers, R.A. Cowley, G. Dolling, Phys. Rev. 167 (1968) 510.
[18] Y. Ikedo, J. Sugiyama, H. Nozaki, H. Itahara, J.H. Brewer, E.J. Ansaldo, G.D. Morris, D. Andreica, A. Amato, Phys. Rev. B 75 (2007) 054424.
[19] E.P. Wohlfarth, Ferromagnetic Materials, vol. 1, North-Holland, Amsterdam, 1980 (and references therein).
[20] D.L. Peng, K. Sumiyama, T.J. Konno, T. Hihara, S. Yamamuro, Phys. Rev. B 60 (1999) 2093;
D.L. Peng, K. Sumiyama, T. Hihara, S. Yamamuro, T.J. Konno, Phys. Rev. B 61 (2000) 3103.
[21] A.N. Dobrynin, D.N. Ievlev, C. Hendrich, K. Temst, P. Lievens, U. Hörmann, J. Verbeeck, G. Van Tendeloo, A. Vantomme, Phys. Rev. B 73 (2006) 245416.
[22] V. Skumryev, S. Stoyanov, Y. Zhang, G. Hadjipanayis, D. Givord, J. Nogués, Nature 423 (2003) 850.
[23] J.A. De Toro, J.P. Andrés, J.A. González, P. Muñiz, T. Muñoz, P.S. Normile, J.M. Riveiro, Phys. Rev. B 73 (2006) 094449.
[24] H. Ouyang, K.-W. Lin, C.–C. Liu, S.–C. Lo, Y.-M. Tzeng, Z.–Y. Guo, J. van Lierop, Phys. Rev. Lett. 98 (2007) 097204.